Can freezing cause floods on Mars?

Chi-yuen Wang,[1] Michael Manga,[1] and Jeffrey C. Hanna[2]

Received 18 July 2006; revised 30 August 2006; accepted 7 September 2006; published 27 October 2006.

[1] Floodwaters on Mars likely originated from aquifers confined below a cryosphere. We use an analytical solution to examine freezing-induced pressurization as a mechanism for releasing groundwater. The results suggest that freezing of an aquifer of global extent under the optimal conditions, i.e., perfectly confined and with low compressibility and high permeability relative to the terrestrial analogs, can release enough floodwaters to carve an individual outflow channel, but not to explain the large total flood volume required to form the all of the outflow channels. It can also produce discharges comparable to those required for carving the outflow channels by repeated floods. **Citation:** Wang, C.,M. Manga, and J. C. Hanna (2006), Can freezing cause floods on Mars?, *Geophys. Res. Lett.*, *33*, L20202, doi:10.1029/2006GL027471.

1. Introduction

[2] The outflow channels on Mars have long been assumed to form by catastrophic releases of groundwater from the Martian subsurface [e.g., *Carr*, 1979]. The mechanisms by which groundwater is released, however, remain a matter of debate [*Carr*, 1996; *Clifford and Parker*, 2001; *Wang et al.*, 2005; *Hanna and Phillips*, 2005, 2006]. One hypothesis [e.g., *Carr*, 2000] assumes that a rapid decrease of surface temperature and heat flow caused downward freezing of a Martian aquifer and trapped groundwater between a thickening cryosphere and an impervious basement; pore pressure in the aquifer increased to exceed lithostatic pressure at the base of the cryosphere, leading to eruption of groundwater to produce floods. Using numerical simulations, *Hanna and Phillips* [2005] showed that a negative feedback between pore pressure and aquifer properties may make it difficult for the mechanism to generate lithostatic pore pressures if the aquifer is laterally unconfined. Here we derive an analytical model for confined aquifers that allows us to quantify the effect of aquifer freezing on floods.

2. Pressurization of the Martian Aquifer by Progressive Freezing

[3] Meteoritic bombardment and volcanism on early Mars may have created a thick layer of regolith and jointed basalt that was hydrologically connected and became confined beneath a global cryosphere during Hesperian [e.g., *Carr*, 1996; *Clifford and Parker*, 2001]. Groundwater expelled from the freezing aquifer would flow to fill unsaturated pores, and conditions may have developed where local, regional and even continental scale aquifers became saturated and confined both vertically and laterally by differences in cryosphere thickness and the depth of hydraulic continuity.

[4] As a result of the volumetric expansion of water upon freezing and assuming ice lenses and frost heave do not form freezing in a saturated aquifer will expel ~9% of the pore water from the frozen portion and force it into the unfrozen portion of the aquifer, causing the pore pressure to rise. We assume that the aquifer, prior to the onset of freezing, was in hydrostatic equilibrium. Thus the increase in pore pressure due to freezing is the *excess* pore pressure, denoted by P_{ex}. The expelled water is related to the rate of increase of pore pressure by [*Bredehoeft and Hanshaw*, 1968]:

$$S_s \frac{\partial P_{ex}}{\partial t} = \nabla \cdot \left(\frac{\rho_w g k}{\mu} \nabla P_{ex} \right) + \rho_w g \Gamma, \tag{1}$$

where k is the permeability of the aquifer, μ and ρ_w, respectively, are the viscosity and density of water, g the gravitational acceleration, S_s the specific storage which is a function of both depth z and pore pressure P_p,

$$S_s(z, P_p) = \rho_w g \left[n(z, P_p) \beta_w + \beta_m(z, P_p) \right], \tag{2}$$

where n the porosity of the aquifer, β_w and β_m are the compressibility of water and the aquifer matrix, respectively. Γ is the 'source' of water per unit volume and is related to the rate of freezing $d\tilde{z}/dt$ by

$$\Gamma = \frac{0.09 n(\tilde{z}, P_p)}{H - \tilde{z}} \frac{d\tilde{z}}{dt}, \tag{3}$$

where $\tilde{z}$ is the depth of the freezing front and H is the base of the aquifer where porosity is eliminated by various geologic processes [*Palciauskas and Domenico*, 1989; *Renard et al.*, 2000; *Travis et al.*, 2003; *Hanna and Phillips*, 2005]. Estimates of H are poorly constrained but *Carr* [1996] suggest $H \sim 10$ km, and *Hanna and Phillips* [2005] suggest an upper limit of 10 to 20 km.

[5] We consider a horizontal aquifer with its vertical dimension very much smaller than its lateral dimension (inset of Figure 1). Since the aquifer is assumed to be confined on all sides, large-scale horizontal flow is absent. Since the rate of freezing is much smaller than the rate of vertical diffusion of the pore pressure generated at the front of the thickening cryosphere [*Hanna and Phillips*, 2005], the entire remaining aquifer responds essentially instantaneously and large-scale vertical flow is also absent. Thus (1) reduces to

$$\overline{S}_s \frac{dP_{ex}}{dt} = \rho_w g \Gamma \tag{4}$$

[1]Department of Earth and Planetary Science, University of California, Berkeley, California, USA.
[2]Department of Earth, Atmospheric, and Planetary Sciences, Massachusetts Institute of Technology, Cambridge, Massachusetts, USA.

0094-8276/06/2006GL027471$05.00

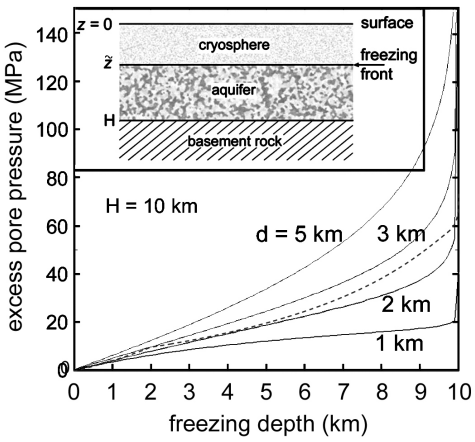

Figure 1. Excess pore pressure as a function of the freezing front depth, calculated with $H = 10$ km and d from 1 to 5 km. Dashed line represents pressures generated using the hydrological model of *Hanna and Phillips* [2005].

where $\overline{S}_s$ is the average storage of the aquifer beneath the freezing front (inset of Figure 1):

$$\overline{S}_s = \frac{1}{H-\tilde{z}}\int_{\tilde{z}}^{H} S_s(\zeta, P_p)\,d\zeta = \frac{\rho_w g}{H-\tilde{z}}\int_{\tilde{z}}^{H}\left[n(\zeta, P_p)\beta_w + \beta_m(\zeta, P_p)\right]d\zeta. \quad (5)$$

If the rate of freezing is known as a function of time, (4) may be integrated to yield the pore-pressure history. But the freezing history of the Martian aquifer is uncertain [e.g., *Clifford and Parker*, 2001; *Hanna and Phillips*, 2005]; we thus examine instead the pressurization as a function of the freezing depth, i.e.,

$$\frac{dP_{ex}}{d\tilde{z}} = \frac{0.09\,n(\tilde{z}, P_p)}{\int_{\tilde{z}}^{H}\left[n(\zeta, P_p)\beta_w + \beta_m(\zeta, P_p)\right]d\zeta}. \quad (6)$$

3. Aquifer Properties

[6] Since n and β_m depend on pore pressure as well as on depth, (6) is nonlinear and generally requires numerical solution [e.g. *Hanna and Phillips*, 2005]. A common porosity model assumes that porosity decreases exponentially with depth [*Athy*, 1930; *Binder and Lange*, 1980; *Clifford*, 1993; *Clifford and Parker*, 2001]:

$$n(z) = n_o \exp(-z/d), \quad (7)$$

where n_o is the porosity at the surface ($z = 0$) and d is a scaling parameter. For the Martian megaregolith, *Clifford* [1981] obtained $d = 2.8$ km. *Hanna and Phillips* [2005] developed a detailed constitutive model for the Martian crust, with several categories of materials each with distinct hydraulic properties. Nevertheless, the above model with $d = 3$ km agrees with Hanna and Phillips' porosity model within the range of uncertainty to a depth of ~5 km [*Hanna and Phillips*, 2005, Figure 4] and differs from it by less than 0.02 on average below 5 km.

[7] Since porosity depends not only on depth but also on pore pressure, we introduce an 'effective depth' as

$$z_{eff} \equiv \frac{P_{eff}}{\rho_c g} = \frac{P_{litho} - \alpha P_p}{\rho_c g} = z - \frac{\alpha P_p}{\rho_c g}, \quad (8)$$

where P_{eff} is the effective pressure, P_{litho} the lithostatic pressure ($P_{litho} \equiv \rho_c g z$), P_p is the pore pressure and is equal to the sum of the hydrostatic pressure ($P_{hydro} \equiv \rho_w g z$) and the excess pore pressure P_{ex}, ρ_c the average density of the cryosphere, and α the Biot-Willis parameter. Thus the initial porosity profile (i.e., prior to pressurization) at hydrostatic pressure is given by

$$n\left(z, z_{eff}^{hydro}\right) = n_o \exp\left(-\frac{z_{eff}^{hydro}}{d}\right) = n_o \exp\left(\frac{-(\rho_c - \alpha\rho_w)z}{\rho_c d}\right) = n_o \exp\left(\frac{-z}{\tilde{d}}\right) \quad (9)$$

where n_o is the uncompressed porosity at the surface and $\tilde{d} \equiv d/(1 - \alpha\rho_w/\rho_c)$ is the scaling parameter at hydrostatic pressure.

[8] Estimation of the decrease in porosity with depth is commonly made on the assumption of elastic compression [*Clifford*, 1993]. However, the mechanical compaction of porous sediments is largely irreversible [e.g., *Lambe and Whitman*, 1969; *Neuzil*, 2003; *Ingebritsen et al.*, 2006]. Compressibility values estimated from the porosity data ignoring the non-elastic changes in the pore volume with depth are generally an order of magnitude greater than values obtained from direct measurements [*Deming*, 2002]. Thus for estimating the porosity and compressibility of the Martian aquifer during pressurization, we use a scaling parameter of $\gamma\, d$, where γ is ~10, while keeping the same exponential form of the equation, following an approach adopted by *Shi and Wang* [1986] in the analysis of sediment decompression under excess pore pressure. The porosity at depth z and excess pore pressure P_{ex} is then

$$n(z, z_{eff}) = n\left(z, z_{eff}^{hydro}\right)\exp\left(\frac{\alpha P_{ex}}{\rho_c g \gamma d}\right) = n_o \exp\left[-\left(1 - \frac{1}{\gamma}\right)\frac{z}{\tilde{d}}\right]\exp\left(-\frac{z_{eff}}{\gamma d}\right), \quad (10)$$

and the porosity at lithostatic pore pressure (just before the occurrence of hydrofracturing) is:

$$n\left(z, z_{eff}^{litho}\right) = n_o \exp\left[-\left(1 - \frac{1}{\gamma}\right)\frac{z}{\tilde{d}}\right]\exp\left(-\frac{z_{eff}^{litho}}{\gamma d}\right) = n_o \exp\left(-\frac{z}{\tilde{d}}\right)\exp\left(\frac{\tilde{z}}{\gamma d}\right). \quad (11)$$

Assuming that the solid grains are incompressible we express compressibility as

$$\beta_m(z,z_{eff}) = -\frac{1}{V}\frac{dV}{dP_{eff}} \approx -\frac{1}{V}\frac{dV_{pore}}{dP_{eff}} = -\frac{1}{1-n(z,z_{eff})}\frac{dn}{dP_{eff}}$$
$$= \frac{1}{\rho_c g\gamma d}\frac{n(z,z_{eff})}{1-n(z,z_{eff})}$$
$$= \frac{1}{\rho_c g\gamma d}\frac{n_o \exp\left[-\left(1-\frac{1}{\gamma}\right)\frac{z}{d}\right]\exp\left(-\frac{z_{eff}}{\gamma d}\right)}{1-n_o \exp\left[-\left(1-\frac{1}{\gamma}\right)\frac{z}{d}\right]\exp\left(-\frac{z_{eff}}{\gamma d}\right)} \quad (12)$$

where V is the bulk volume of the aquifer and V_{pore} the pore volume. Equations (10) and (12) approximate the porosity and compressibility model of *Hanna and Phillips* [2005] for $n_0 = 0.15$, $d = 3$ km, and $\gamma = 5$.

[9] Given (10) and (12), and realizing that the remaining aquifer responds to freezing essentially instantaneously so that the excess pore pressure is constant in space at any given time (though its value varies with time), the denominator of (6) may be explicitly expressed as:

$$\int_{\tilde{z}}^{H}\left[n(\zeta,P_p)\beta_w + \beta_m(\zeta,P_p)\right]d\zeta = n_o\beta_w\tilde{d}$$
$$\cdot \exp\left(\frac{\alpha P_{ex}}{\rho_c g\gamma d}\right)\left[\exp\left(-\frac{\tilde{z}}{\tilde{d}}\right) - \exp\left(-\frac{H}{\tilde{d}}\right)\right]$$
$$+ \frac{\tilde{d}}{\rho_c g d}\ln\left(\frac{1-n_o\exp\left(\frac{\alpha P_{ex}}{\rho_c g\gamma d}-\frac{H}{\tilde{d}}\right)}{1-n_o\exp\left(\frac{\alpha P_{ex}}{\rho_c g\gamma d}-\frac{\tilde{z}}{\tilde{d}}\right)}\right). \quad (13)$$

Given (13) we may integrate (6) numerically to evaluate the pressurization of the aquifer as a function of freezing depth and the assumed parameters.

[10] If the pore pressure increases to lithostatic at the base of the cryosphere, rupture will occur, pressurized water will erupt to the surface, and the pressure will return to hydrostatic. The amount of water released during an rupturing event can be calculated from the difference in the pore volume between the lithostatic and hydrostatic pore pressures, taking into account the expansion of the water during the pressure release:

$$v(\tilde{z}) = \exp(\beta_w,\tilde{P}_{ex})\cdot\int_{\tilde{z}}^{H} n\left(\zeta,\zeta_{eff}^{litho}\right)d\zeta - \int_{\tilde{z}}^{H} n\left(\zeta,\zeta_{eff}^{hydro}\right)d\zeta$$
$$= n_o\tilde{d}\left[1-\exp(\beta_w\tilde{P}_{ex})\exp\left(\frac{\tilde{z}}{\gamma d}\right)\right]\left[\exp\left(-\frac{H}{\tilde{d}}\right) - \exp\left(\frac{\tilde{z}}{\tilde{d}}\right)\right] \quad (14)$$

where $\tilde{P}_{ex}$ is the excess pore pressure at the time of rupture.

4. Results and Discussion

[11] Of the parameters in the above equations, H and d are the mostly poorly constrained; so we consider ranges of H and d from 1 to 10 km. The values of α range from 0.7 to 1 for porous sedimentary rocks [*Wang*, 2000, Appendix C], which reduce to 1 if the solid grains are incompressible. To be consistent with the earlier assumption that the solid grains in the aquifer are incompressible, we choose $\alpha = 1$. For the other parameters we use $n_o = 0.3$, $\rho_c = 2200$ kg/m^3 and $g = 3.7$ m/s^2. Figure 1 shows the calculated excess pore pressure (P_{ex}) as a function of $\tilde{z}$ for selected H and d, as well as for the model of *Hanna and Phillips* [2005]. For a given H, the curves rise more steeply with greater d, reflecting a decreasing compressibility (or increasing stiffness) of the aquifer matrix with increasing d. Along each curve, the slope increases with increasing $\tilde{z}$, reflecting a decreasing compliance with decreasing aquifer thickness.

[12] Figure 2a shows the depth of freezing required for P_p to reach lithostatic as a function of H and d. The curves flatten in the range of d-values where the entire aquifer needs to be frozen to raise the pore pressure to lithostatic. Figure 2b shows the ratio of z and H as a function of H and d. The area below the line with $z/H = 1$ corresponds to that in Figure 2a where the curves are flat. Figure 2c shows the amount of water released from a rupture event. Significant amount of water (1 to 2 m per unit area) may be released when the cryosphere thickens to 1 to 6 km if $d > \sim$4 km and H between 1.5 to 6 km; repeated rupturing events may release more water. For comparison, the hydrological models of *Hanna and Phillips* [2005] assuming aquifer thicknesses of 5 and 10 km predict superlithostatic pore pressures after thickening of the cryosphere to 0.6 and 9.6 km, subsequently releasing 5.9 and 4.4 m of water per unit area, respectively.

[13] Estimates of the volume of floodwater required to carve the outflow channels are extremely uncertain. For floods with high sediment load, *Carr* [1996] estimated volumes up to 3×10^5 km^3 for individual floods and 6×10^6 km^3 for all the circum-Chryse channels, similar to the estimate of *Rotto and Tanaka* [1992]. Thus under the optimal condition (v = 2 m, Figure 2c) freezing of an aquifer of global extent would release 3e5 km^3, enough to carve an individual channel but significantly short of the volume required to carve all of the outflow channels. However, the assumed aquifer size is an upper bound; the calculated flood volumes would be reduced if the aquifers were not laterally as well as vertically confined [*Hanna and Phillips*, 2005] and if the commonly assumed values for H (10 to 20 km) and d (3 km) are used.

[14] To estimate the discharge we assume a simplified geometry in which a square aquifer of size $L \times L$ is bounded on all sides except the ruptured edge L', allowing the aquifer to drain freely in the horizontal direction. This geometry is most appropriate to the flow of water in an aquifer that is penetrated by a deep canyon, such as Echus Chasma at the source of Kasei Valles, or the main Valles Marineris canyons. The discharge through the ruptured edge is given by Darcy's law:

$$Q = -\frac{k}{\mu}\frac{\partial P_{ex}}{\partial x}A \quad (15)$$

where A is the area of the ruptured surface, i.e., the area of discharge, normal to x, and is equal to $(H - z)\,L'$, where $(H - z)$ is the thickness of the unfrozen aquifer, and $\partial P_{ex}/\partial x$ is the horizontal gradient of the excess pore pressure at the rupture. Since the duration of flow is short, pressurization due to freezing is negligible (i.e., Γ in (1) is zero). As pore pressure decreases from lithostatic to hydrostatic, S_s and k both change; thus (1) is nonlinear and requires numerical solution [e.g., *Hanna and Phillips*, 2005]. To simplify the

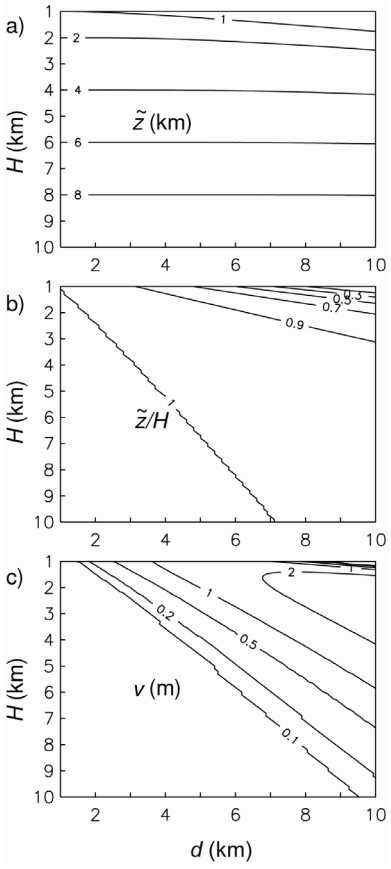

Figure 2. (a) Depth of freezing required to raise the pore pressure to lithostatic as a function of H and d. Where the curves are flat in this diagram, the entire aquifer needs to be frozen to raise pore pressure to lithostatic. (b) Ratio between the required depth for freezing (z) and the initial thickness of the aquifer (H) and d. The area below the line with z/H = 1 corresponds to that in Figure 2a where the curves are flat. (c) Volume of expelled water per unit area during the rupture of the cryosphere as a function of H and d.

problem we estimate the upper bound of the discharge by assuming the parameter values at the lithostatic pore pressures. With the boundary conditions $P_{ex} = 0$ at $x = L$ and no flow at $x = 0$, the solution for 1-D flow through the aquifer is [*Carslaw and Jaeger*, 1959, p. 97],

$$Q(t) = \frac{2k\tilde{P}_{ex}}{\mu L}(H - \tilde{z})L' \sum_{m=0}^{\infty} \exp\left(-\frac{\rho_w g \bar{k}(2m+1)^2\pi^2}{4\mu \bar{S}_s L^2}t\right) \quad (16)$$

where $\tilde{P}_{ex}$ is the pore pressure just prior to the occurrence of hydrofracturing, and $\bar{k}$ and $\bar{S}_s$ are, respectively, the vertically averaged permeability and specific storage in the unfrozen aquifer. At the lithostatic pore pressure, $\bar{S}_s$ may be calculated by using equations (5) and (13) and $\bar{k}$ may be calculated by using the Kozeny-Carman relation

$$\bar{k}\left(z, z_{eff}\right) = \frac{\bar{n}\left(z, z_{eff}^{litho}\right)^3}{5s_o^2\left(1 - \bar{n}\left(z, z_{eff}^{litho}\right)\right)^2} \quad (17)$$

where $\bar{n}(z, z_{eff}^{litho})$ is the vertically averaged porosity at lithostatic pore pressure given in (9) and s_o is the solid surface exposed to water per unit volume of the aquifer. We note that the Kozeny-Carmen relation was derived to relate the permeability of sandstones to the porosity [*Dullien*, 1992]. Assuming $n_o = 0.3$ and $k_o = 10^{-9}$ m^2 [*Manga*, 2004], we have $s_o \sim 3 \times 10^3$ m^2/m^3. The permeability of 10^{-9} m^2 is a very high value for geologic material but is typical of rubbly, unaltered volcanic rocks of the Kilauea Volcano and the Oregon Cascades; the specific surface of 3×10^3 m^2/m^3 corresponds to regoliths with an average grain size of gravels. *Hanna and Phillips* [2005], on the other hand, suggested $k_0 = 10^{-11}$ m^2, which corresponds to $s_0 \sim 3 \times 10^4$ m^2/m^3.

[15] For rocks with parallel fractures, a cubic law $k = (Nb^3)/12 = n^3/(12N^2)$ may be used [*Snow*, 1968], where N is the number of fractures per unit distance, b the fracture aperture and $n = N\,b$. If $N = 10$ m^{-1} (i.e., fracture spacing of 0.1 m), a permeability of 10^{-9} m^2 corresponds to $b \sim 10^{-3}$ m and $n \sim 0.01$; thus little water will be available. If $n \sim 0.3$ instead, a permeability of 10^{-9} m^2 corresponds to $N \sim 10^3$ m^{-1}, or a fracture spacing down to the diameter of sand; thus the cubic law becomes almost identical to the Kozeny-Carmen relation. We use (17) in the following calculation.

[16] We consider two end-member aquifer sizes: $L = L'$ = 300 km and 10,000 km. The upper limit corresponds to the extreme case of a relatively uniform aquifer overlain by a global blanket of impervious cryosphere. For each aquifer size, we consider H, d = 1, 3, 5 and 10 km. All other things being equal, the calculated discharges are proportional to L' and decline exponentially with time. With L' = 300 km, the calculated discharge ranges from $\sim 5 \times 10^2$ m^3/s ($H = d$ = 1 km) to $\sim 5 \times 10^5$ m^3/s (H = 3 km, d = 10 km) at the end of the first hour after eruption, and declines to $\sim$50 m^3/s and $\sim 5 \times 10^4$ m^3/s, respectively, at the end of the first month ($\sim 10^{-1}$ yr) after eruption. With L' = 10,000 km, on the other hand, the calculated discharge ranges from $\sim 10^4$ m^3/s ($H = d$ = 1 km) to $\sim 10^7$ m^3/s (H = 3 km, d = 10 km) at the end of the first hour after eruption, and declines to $\sim 10^3$ m^3/s and $\sim 10^6$ m^3/s, respectively, at the end of the first month after eruption. A drastic decline in the discharge occurs at a time proportional to L^2, which is $\sim 10^2$ yr for L = 300 km (Figure 3) and $\sim 10^5$ yr for L = 10,000 km. Discharges an order of magnitude lower than those in Figure 3 would be expected for the lower permeability model of *Hanna and Phillips* [2005].

[17] *Robinson and Tanaka* [1990] suggested an upper limit 1.2 to 3.5×10^9 m^3/s for Kasei Vallis, assuming bankfull discharges. However, using high-resolution data for Kasei Valles and Athabasca Valles, respectively, *Williams et al.* [1999] and *Burr et al.* [2002] identified incised channels, fluvial terraces and cross-truncation of longitudinal grooves within the outflow channels, and argued that the channels may have formed by repeated floods, each with much smaller peak discharges (8×10^4 to 2×10^7 m^3/s for Kasei Valles [*Williams et al.*, 1999]; $\sim 10^6$ m^3/s for Athabasca Valles [*Burr et al.*, 2002]). These lower discharges are comparable to those produced by the freezing aquifer model under optimal conditions.

[18] In summary, we find that under the optimal conditions, freezing of the Martian aquifer can release enough

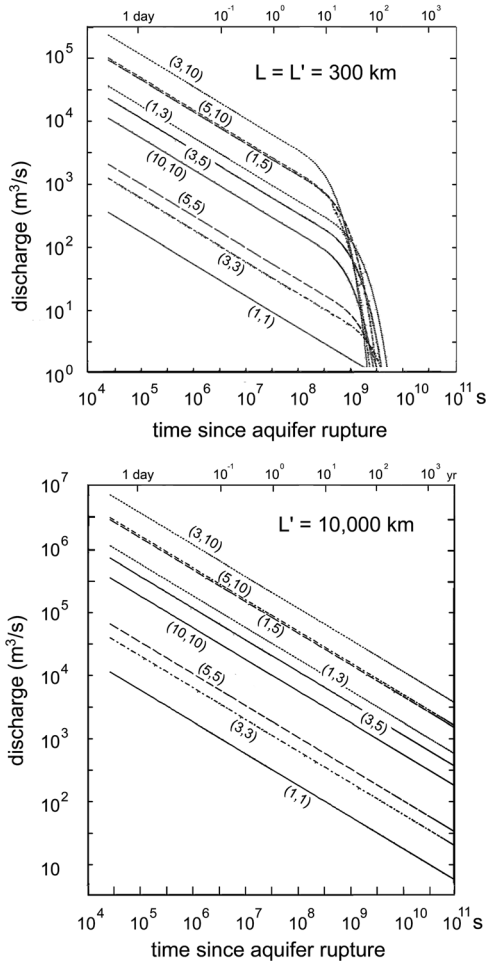

Figure 3. Calculated discharges (m^3/s) as function of time (s, on the lower edge of each diagram) for ruptured aquifers of different sizes. The numbers in parentheses correspond to values of (H, d) in km.

flood water to the surface to produce individual floods, but not to explain the large volumes required to explain the outflow channels as a group. Discharges comparable to those inferred for carving the outflow channels by repeated floods can also be produced under these conditions. Large uncertainties in the parameters H and d, the size of the aquifer and the estimates of flood volumes and discharges required to carve the outflow channels prevent a more definitive answer to the question posed in the title of the paper.

[19] **Acknowledgments.** We thank Steve Ingebritsen, Steve Clifford and an anonymous reviewer for their comments. Work was supported in part by NASA Astrobiology Institute (NNA04CC02A).

References

Athy, L. F. (1930), Density, porosity and compaction of sedimentary rocks, *AAPG Bull.*, *14*, 1–24.

Binder, A. B., and M. A. Lange (1980), On the thermal history, thermal state, and related tectonism of a Moon of fission origin, *J. Geophys. Res.*, *85*, 3194–3208.

Bredehoeft, J. D., and B. B. Hanshaw (1968), On the maintenance of anomalous fluid pressures: I. Thick sedimentary sequences, *Geol. Soc. Am. Bull.*, *79*, 1097–1106.

Burr, D. M., et al. (2002), Repeated aqueous flooding from the Cerberus Fossae: Evidence for very recently extant, deep groundwater on Mars, *Icarus*, *159*, 53–73.

Carr, M. H. (1979), Formation of Martian flood features by release of water from confined aquifers, *J. Geophys. Res.*, *87*, 6781–6790.

Carr, M. H. (1996), *Water on Mars*, 229 pp., Oxford Univ. Press, New York.

Carr, M. H. (2000), Martian oceans, valleys, and climate: New insights from Mars Global Surveyor, *Astron. Geophys.*, *41*, 3.20–3.26.

Carslaw, H. S., and J. C. Jaeger (1959), *Conduction of Heat in Solids*, 510 pp., Oxford Univ. Press, New York.

Clifford, S. M. (1981), A pore volume estimate of the Martian megaregolith based on a lunar analog, in *3rd International Colloquium on Mars, LPI Contrib. 441*, pp. 46–48, Lunar and Planet. Inst., Houston, Tex.

Clifford, S. M. (1993), A model for the hydrologic and climatic behavior of water on Mars, *J. Geophys. Res.*, *98*, 10,973–11,016.

Clifford, S. M., and T. J. Parker (2001), The evolution of the Martian hydrosphere: Implications for the fate of a primordial ocean and the current state of the northern plains, *Icarus*, *154*, 40–79.

Deming, D. (2002), *Introduction to Hydrogeology*, 468 pp., McGraw-Hill, New York.

Dullien, F. A. L. (1992), *Porous Media, Fluid Transport and Pore Structure*, 574 pp., Elsevier, New York.

Hanna, J. C., and R. J. Phillips (2005), Hydrological modeling of the Martian crust with application to the pressurization of aquifers, *J. Geophys. Res.*, *110*, E01004, doi:10.1029/2004JE002330.

Hanna, J. C., and R. J. Phillips (2006), Tectonic pressurization of aquifers in the formation of Mangala and Athabasca Valles, Mars, *J. Geophys. Res.*, *111*, E03003, doi:10.1029/2005JE002546.

Ingebritsen, S., W. Sanford, and C. Neuzil (2006), *Groundwater in Geologic Processes*, 536 pp., Cambridge Univ. Press, New York.

Lambe, T. M., and R. V. Whitman (1969), *Soil Mechanics*, 553 pp., John Wiley, Hoboken, N. J.

Manga, M. (2004), Martian floods at Cerberus Fossae can be produced by groundwater discharge, *Geophys. Res. Lett.*, *31*, L02702, doi:10.1029/2003GL018958.

Neuzil, C. E. (2003), Hydromechanical coupling in geologic processes, *Hydrogeol. J.*, *11*, 41–83.

Palciauskas, V. V., and P. A. Domenico (1989), Fluid pressures in deforming porous rocks, *Water Resour. Res.*, *25*, 203–213.

Renard, F., J. Gratier, and B. Jamtveit (2000), Kinetics of crack-sealing, intergranular pressure solution, and compaction around active faults, *J. Struct. Geol.*, *22*, 1395–1407.

Robinson, M. S., and K. L. Tanaka (1990), Magnitude of a catastrophic flood event at Kasei Valles, Mars, *Geology*, *18*, 902–905.

Rotto, S. L., and K. L. Tanaka (1992), Chryse Planitia region, Mars: Channeling history, flood volume estimates, and scenarios for bodies of water in the northern plains, paper presented at Workshop on the Martian Surface and Atmosphere Through Time (MSATT), Lunar and Planet. Inst., Houston, Tex.

Shi, Y., and C.-Y. Wang (1986), Pore pressure generation in sedimentary basins: Overloading versus aquathermal, *J. Geophys. Res.*, *91*, 2153–2162.

Snow, D. T. (1968), Rock fracture spacing, openings and porosities, *Proc. Am. Soc. Civ. Eng.*, *94*, 73–91.

Travis, B. J., N. D. Rosenberg, and J. N. Cuzzi (2003), On the role of widespread subsurface convection in bringing liquid water close to Mars surface, *J. Geophys. Res.*, *108*(E4), 8040, doi:10.1029/2002JE001877.

Wang, C.-Y., M. Manga, and A. Wong (2005), Floods on Mars released from groundwater by impact, *Icarus*, *175*, 551–555.

Wang, H. F. (2000), *Theory of Linear Poroelasticity*, Princeton Univ. Press, Princeton, N. J.

Williams, R. M., R. J. Phillips, and M. C. Malin (1999), Flow rates and duration within Kasei Valles, Mars: Implications for the formation of a Martian ocean, *Geophys. Res. Lett.*, *27*, 1073–1076.

J. C. Hanna, Department of Earth, Atmospheric, and Planetary Sciences, Massachusetts Institute of Technology, Cambridge, MA 02139, USA.

M. Manga and C. Wang, Department of Earth and Planetary Science, University of California, Berkeley, CA 94720-4767, USA. (chiyuen@bekeley.edu)